Nuclear Instruments and Methods in Physics Research A 862 (2017) 25–30

Contents lists available at ScienceDirect

Nuclear Instruments and Methods in Physics Research A

journal homepage: www.elsevier.com/locate/nima

Measurement of basic characteristics and gain uniformity of a triple GEM detector

Rajendra Nath Patra [a,*], Rama N. Singaraju [a], Saikat Biswas [b], Zubayer Ahammed [a], Tapan K. Nayak [a,c], Yogendra P. Viyogi [a]

[a] Variable Energy Cyclotron Centre, HBNI, Kolkata 700064, India
[b] Bose Institute, Department of Physics and CAPSS, Kolkata 700091, India
[c] CERN, Geneva 23, Switzerland

ARTICLE INFO

Article history:
Received 28 March 2017
Received in revised form
6 May 2017
Accepted 8 May 2017
Available online 9 May 2017

Keywords:
Micro pattern gas detectors
GEM
Gain
Efficiency
Resolution
Uniformity

ABSTRACT

Large area Gas Electron Multiplier (GEM) detectors have been the preferred choice for tracking devices in major nuclear and particle physics experiments. Uniformity over surface of the detector in terms of gain, energy resolution and efficiency is crucial for the optimum performance of these detectors. In the present work, detailed performance study of a 10×10 cm^2 triple GEM detector operated using Ar and CO_2 gas mixtures in proportions of 70:30 and 90:10, has been made by making a voltage scan of the efficiency with ^{106}Ru-Rh β-source and cosmic rays. The gain and energy resolution of the detector were studied using the X-ray spectrum of ^{55}Fe source. The uniformity of the detector has been investigated by dividing the detector in 7×7 zones and measuring the gain and energy resolution at the centre of each zone. The variations of the gain and energy resolution have been found to be 8.8% and 6.7%, respectively. These studies are essential to characterise GEM detectors before their final use in the experiments.

1. Introduction

New generation nuclear and particle physics experiments require charged particle tracking devices with low material budget and excellent position resolutions. For the last several decades, various types of micro-pattern gas detectors (MPGD) have been developed for their use in experiments at major accelerator facilities as well as for applications in imaging technologies. Gas Electron Multiplier (GEM) detectors, developed at CERN in 1997 [1,2], is one of the new generation MPGD, which fulfils the stringent conditions of existing and proposed large scale experiments. With increasing energy and beam luminosity in accelerator facilities, the requirements for detector technologies have been continuously changing. Because of their high rate capability, fast timing, good position resolution and ion suppression features, GEM detectors have widely been chosen as preferred tracking devices in particle and heavy-ion physics experiments [3–5]. Charged particle tracking devices in experiments at Brookhaven National Laboratory [6,7], CERN Large Hadron Collider [8–11], the Facility for Antiproton and Ion Research (FAIR) at GSI [12–14] and future experiments in International Linear Collider (ILC) [15] have chosen GEM detectors.

A GEM foil consists of an insulator made of a 50 μm thick Kapton foil with 5 μm thick copper cladding on both sides and pierced by a regular array of holes. These perforated holes, having typically 70 μm diameter and separated by 140 μm pitch, are arranged in a hexagonal pattern. Depending on the etching method, the holes are single conical or bi-conical. A bias voltage of 350–400 V applied across the GEM foils, provides a very high electric field (~70 kV/cm) in the holes because the field lines are focused in the holes. This creates large gas amplification, up to several thousands. The electrons are collected on an anode, which is the readout plane. Due to the micro-hole structure, excellent spatial resolution (of the order of 100 μm) along with a reasonable time resolution (about 10 ns) can be achieved. Another major advantage of the GEM detectors over other MPGD designs is its ion back flow (IBF) suppression [5] and low discharge probability [16]. In a multistack GEM detector setup, the hole diameter, pitch, electric field across different gas gap can be optimised to minimise the IBF. Discharge probability is reduced as the total electron multiplication is divided into many steps across the holes of the different GEM foils. These features make the GEM detectors suitable candidates for high energy physics experiments.

The GEM detectors, like any other gas detectors, can be characterised in terms of gain, efficiency of detection of charged particles, energy resolution, time resolution, position resolution and rate capability. For a given detector configuration, these parameters vary with applied electric field, gas pressure and

* Corresponding author.
E-mail address: rajendra.nath.patra@cern.ch (R.N. Patra).

http://dx.doi.org/10.1016/j.nima.2017.05.011

temperature. The optimum running conditions are determined depending on the use of the detector. For effective tracking of charged particles, it is essential to have uniform gain over the entire area of the GEM detector. The gain spatial uniformity depends on the quality of GEM foils, uniformity of the holes, fabrication steps and other such quality control parameters. Thus the measurement of gain uniformity forms a basic quality assurance, especially in the case of large area detectors.

In the present study, we have first measured the basic characteristics of a standard triple GEM detector $10 \times 10\ cm^2$ in size. The design of the GEM detector and test setup are presented in the next section. The detector responses to β-source and cosmic rays are discussed in Section 3. Detector characteristics in terms of efficiency, gain, energy and time resolutions are presented in Section 4. We have adopted a new method to measure spatial variations of gain and energy resolution. The respective results are presented and discussed in Section 5. A summary and outlook are given in Section 6.

2. Detector design and experimental setup

The layout of a triple GEM detector is shown in Fig. 1. The detector is constructed by stacking three standard single mask stretched GEM foils manufactured at CERN. Each foil has $10 \times 10\ cm^2$ area, having 70 μm diameter holes arranged in a 140 μm pitch network. In a multi stack GEM detector, the drift, multiplication and induction regions are kept physically separated as shown in the figure. Thus, there is a freedom to design the readout according to the requirement of the experiment. In the present setup, the drift gap, transfer gaps and induction gap are kept as 3-2-2–2 mm, respectively. The drift plane is made of a Kapton foil cladded on one side with a thin (5 μm) layer of copper and the entire detector is kept in a gas tight box. In our setup, the detector has been operated using Argon and CO_2 gas mixtures in proportions of 70:30 and 90:10 at atmospheric pressure.

A voltage difference is applied through a voltage divider resistor chain to produce the required electric field across the GEM foils and in the gas gaps. The resistor chain contains a filter circuit for noise reduction. The design of the resistor chain is made in such a way that a negative high voltage (HV) within the range of 3900–4500 V can be applied. A photograph of the complete triple GEM detector setup along with the voltage divider is shown in Fig. 2.

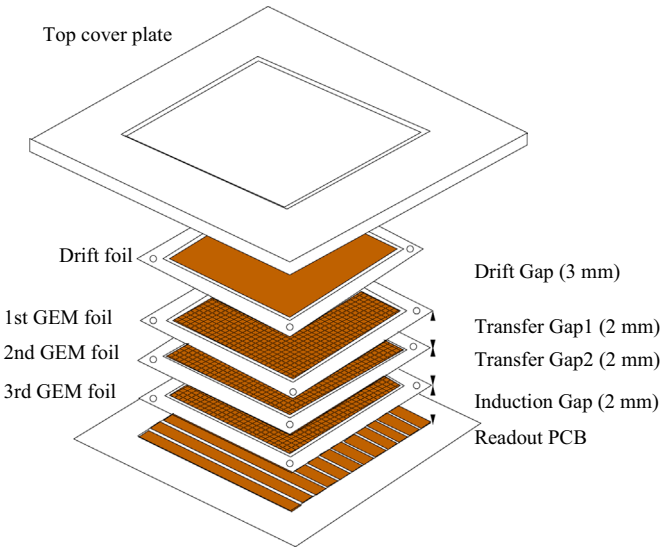

Fig. 1. Geometrical design of the triple GEM detector.

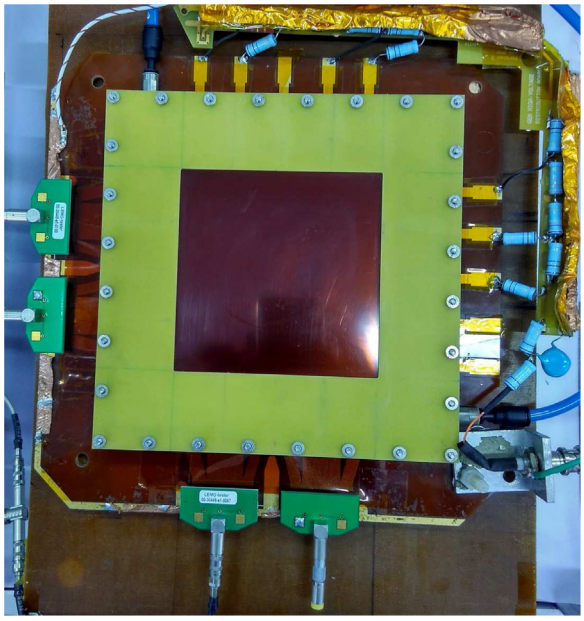

Fig. 2. Photograph of the laboratory setup of the triple GEM detector.

Detector tests are performed by varying the HV. With application of this voltage difference, primary electrons are produced inside the drift gap in presence of incident radiation and those electrons drift towards the first GEM foil. After three stages of charge multiplications within the holes of the GEM foils, the gain of the detector reaches values as high as 10^3–10^5. All electrons drifting to the induction gap are collected in the readout plane. The readout of the detector consists of a base plate with 256 X- and 256 Y- metallic strips. Each of the 256 strips is connected to two 128 pin connectors. A sum-up board adds up signals from 128 readout strips. In total, 4 sum-up boards provide the measured signals.

3. Detector response

The response of the GEM detector has been studied after stabilisation of the gas flow and after minimising the electronics noise [13,17]. The first test of the detector has been performed with cosmic muon. The trigger setup for this study consisted of two cross scintillators placed above the detector and a third scintillator below. A valid trigger consists of coincidence of the signals from all three scintillators. Cosmic muon spectra with gated trigger have been obtained with different HV settings. The top panel of Fig. 3 shows the cosmic muon ADC spectrum taken at 4400 V. The spectrum is fitted with a Landau distribution to have the Most Probable Value (MPV). Studies with cosmic muons take a long time and a faster way to obtain the efficiency is to use a ^{106}Ru-Rh β-source. The trigger setup of three scintillators remains the same as used for cosmic muons. The ADC spectrum corresponding to ^{106}Ru-Rh β-source at 4400 V, is shown in the bottom panel of Fig. 3. In the β-spectrum the MPV value is a bit lower compared to that of cosmic rays.

In order to study the detector gain and energy resolution, the detector has been tested with a ^{55}Fe X-ray source which provides 5.9 keV X-rays. The pulse height spectrum at 4400 V for this source is shown in Fig. 4. The peak at the higher ADC channel corresponds to the 5.9 keV main photo peak and the one to the left is identified as the Argon escape peak.

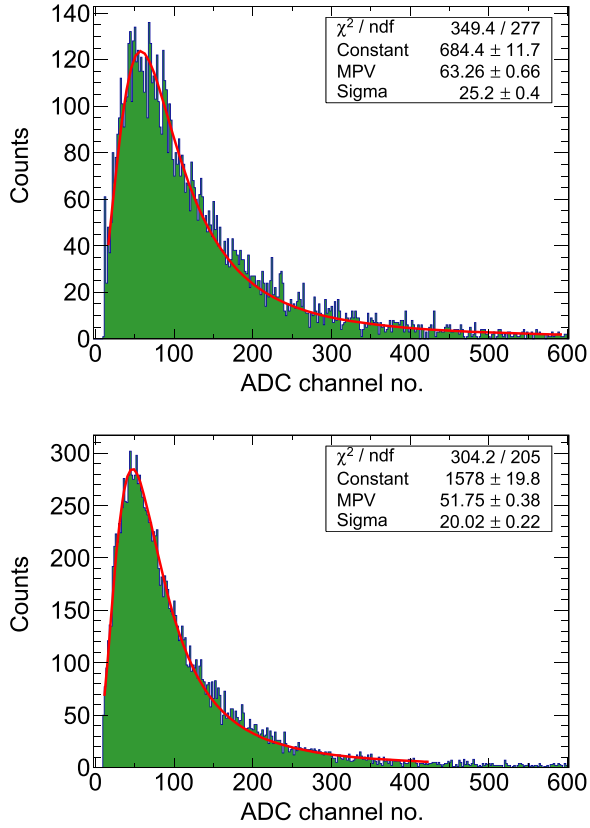

Fig. 3. (top) Cosmic muon and (bottom) ^{106}Ru-Rh β-spectrum at 4400 V for the GEM detector.

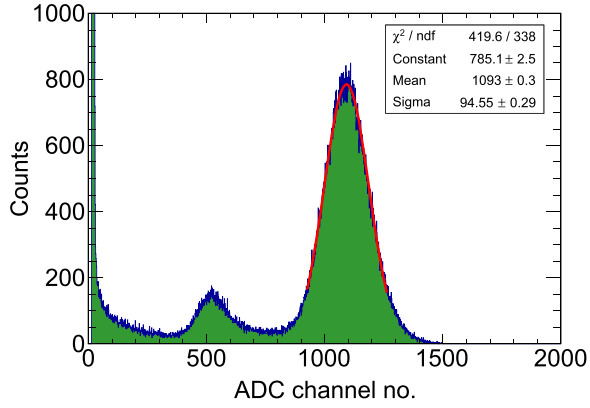

Fig. 4. ^{55}Fe spectrum at 4400 V for the GEM detector.

4. Detector characteristics

Detailed characteristic studies, such as, detector efficiency, gain, energy resolution and time resolution have been performed for the GEM detector using cosmic rays and different radioactive sources. Results of these studies are presented and discussed below.

4.1. Detector efficiency

Efficiency of the GEM detector has been studied with cosmic rays and ^{106}Ru-Rh β-source. For this measurement, trigger was provided by the coincidence signal of a set of three scintillators, as described in the previous section. Number of triggered particles giving signal on the GEM detector yields the efficiency.

Efficiency obtained as a function of applied HV is shown in Fig. 5. The top panel gives the efficiency for Ar-CO_2 gas mixture in 70:30 proportions for cosmic rays and ^{106}Ru-Rh source. The results are very similar. Increasing the HV from 3900 V, the efficiency increases from 20% and beyond 4300 V the efficiency comes to a plateau region at ~95% level. The bottom panel of Fig. 5 shows the efficiency as a function of HV for Ar-CO_2 gas mixture in two proportions, 70:30 and 90:10. These measurements were performed by using the ^{106}Ru-Rh β-source. Similar efficiency values can be achieved for 90:10 gas mixture at a much lower voltage compared to that of 70:30. The optimum detector operation for the 70:30 gas mixture is around 4300 V, whereas for the 90:10 mixture, this voltage is about 3850 V.

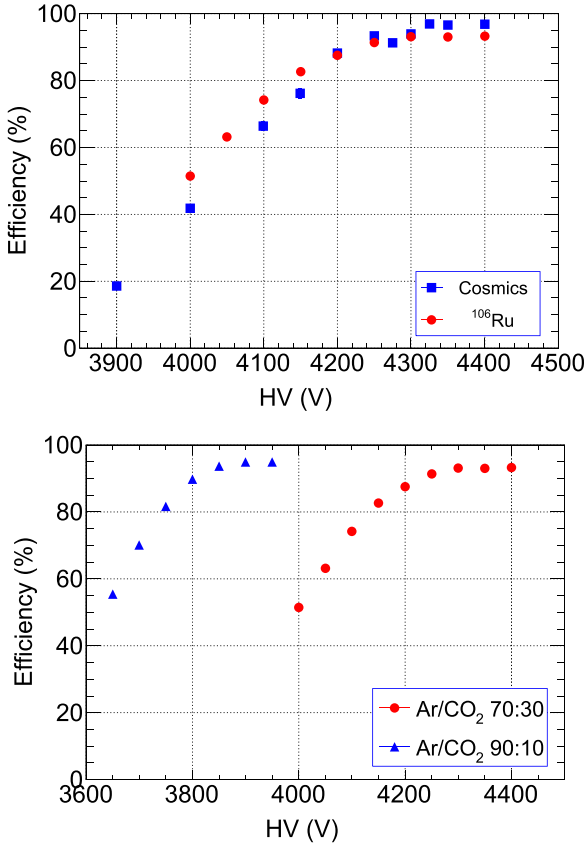

Fig. 5. (top) Efficiency plot for the GEM detector, as a function of HV obtained by using cosmic muon and ^{106}Ru-Rh source with Ar-CO_2 70:30 gas and (bottom) efficiency plot with different Ar-CO_2 gas mixtures, using the ^{106}Ru-Rh β-source.

4.2. Detector gain

One of the important characteristics of any detector is its gain. For this measurement, the detector was tested with a ^{55}Fe X-ray source. The pulse height spectrum for ^{55}Fe has already been shown in Fig. 4. The gain is calculated with the formula:

$$G_{\text{eff}} = \frac{M.\,K_{\text{elec}}}{N_{\text{p}}.\,q_{\text{e}}} \tag{1}$$

where G_{eff} is the effective gain of the detector, M is the mean ADC value of the main peak of the ^{55}Fe spectrum, K_{elec} is the electronics gain factor, N_{p} is the number of primary electrons produced by full energy deposition of 5.9 keV X-ray in the drift volume and q_{e} is the electron charge. Fig. 6 shows the effective gain as a function of HV for two gas mixtures. As expected, gain increases with HV and has an exponential trend. For the 90:10 gas mixture, the gain curve is shifted toward lower HV values with respect to the 70:30 gas mixture.

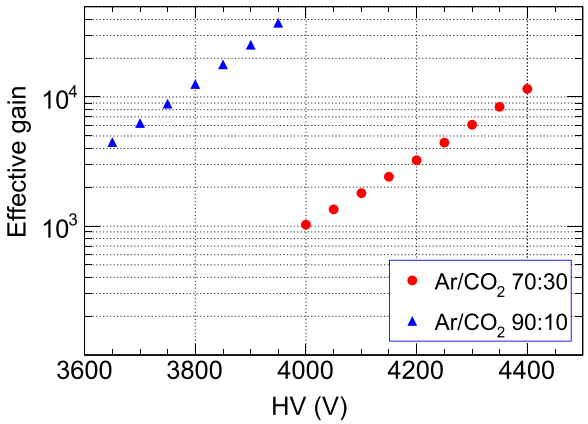

Fig. 6. Effective gain of the GEM detector as a function of HV for the two gas mixtures.

4.3. Energy resolution

The energy resolution of the detector is calculated from the Gaussian fit parameters of the main peak of the ^{55}Fe spectrum. The energy resolution for the two gas mixtures as a function of HV is shown in Fig. 7 in terms of FWHM. The energy resolution shows little variation over the range of voltage studied for both gas mixtures and is about 20% (FWHM).

4.4. Time resolution

Time resolution of GEM detectors is determined by the spread in signal formation time for different events. Time resolution depends on several factors, the most important being the electron drift velocity. Drift velocity depends on the gas type and the electric field value. In the present setup, time resolution with the Ar and CO_2 gas mixture in 70:30 proportion was measured using the ^{106}Ru-Rh β-source. The three-fold scintillator trigger described in the previous section was used as start signal and the signal from the GEM detector processed through a fast amplifier was used as the stop signal. The time difference between the start and the stop signals was measured by an ORTEC 567 Time to Amplitude Converter (TAC).

The time spectrum and the plots for time resolution are shown in the top and bottom panels of Fig. 8, respectively. The tail at the lower end of the time spectrum might be due to the fact that

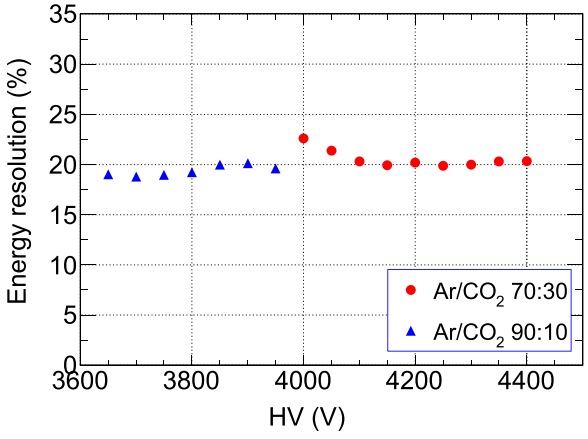

Fig. 7. Energy resolution of the GEM detector as a function of applied HV for the two gas mixtures.

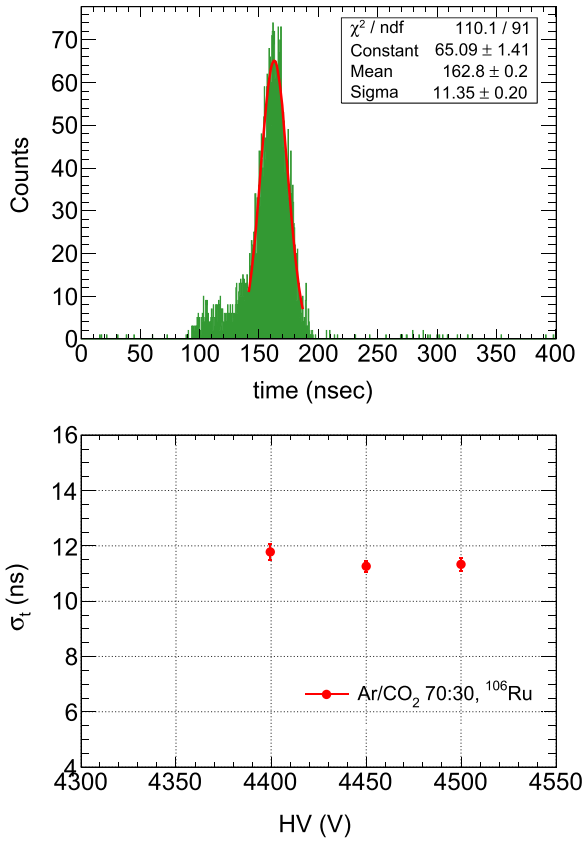

Fig. 8. (top) Time spectrum at 4450 V and (bottom) time resolution as a function of applied HV.

measurements were performed at high gain. Since the gain is high it might be possible to have a signal even if the primary ionisation happens to be in the first transfer gap. In that case the signal will be faster than the majority of the signals whose primaries were generated in the drift area. The results about the time resolution are in agreement with earlier results [2,18].

5. Detector uniformity

New generation high energy physics experiments require large area detectors. The overall performance of these detectors depends on gain uniformity, energy resolution and efficiency over the entire active region. Several factors, like variations in hole diameter, variations in gas gap due to inaccurate stretching, etc., can lead to non-uniformity in the detector [19,20]. Thus it is essential to measure the gain uniformity over the entire surface area. In this work, a method has been used to measure the gain and energy resolution in localised regions and then results obtained across different regions have been compared.

In the setup shown in Fig. 9, a thick perforated PCB is placed above the GEM detector. The 10×10 cm^2 central area of the PCB is divided to 7×7 zones of equal area. The ^{55}Fe source was placed on the centre of each zone and the resulting spectrum was recorded. For each zone, sum-up signals from two associated readout connectors have been read out. For the central zones, however, the charge spreads on all four readout connectors. To have similar data taking conditions for all the zones, it was decided to exclude the central zones. In this process, the gain and energy resolution are measured for 36 zones.

Fig. 10 shows the effective gain values for each zone of the GEM

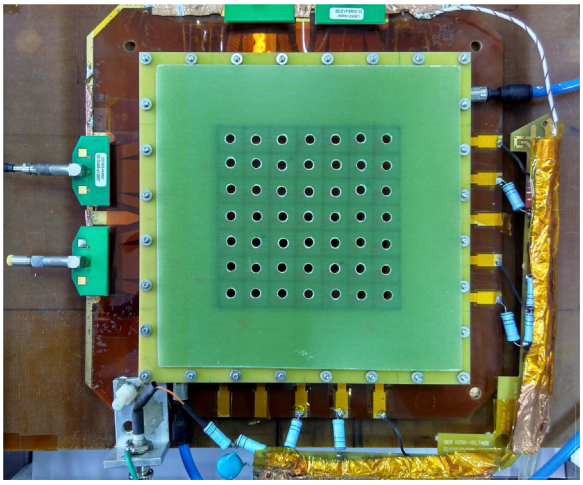

Fig. 9. Test setup for gain and energy resolution uniformity.

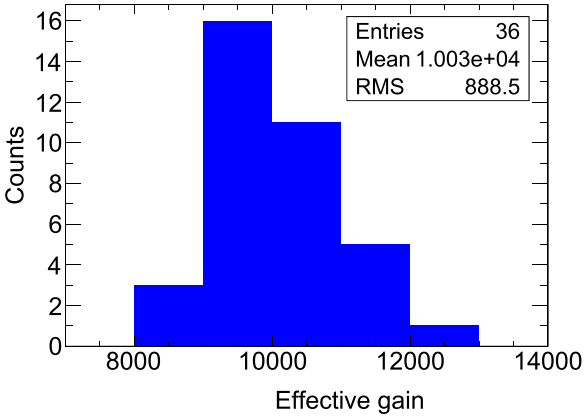

Fig. 10. Distribution of effective gain values for the 36 zones of the GEM detector at an applied voltage of 4400 V.

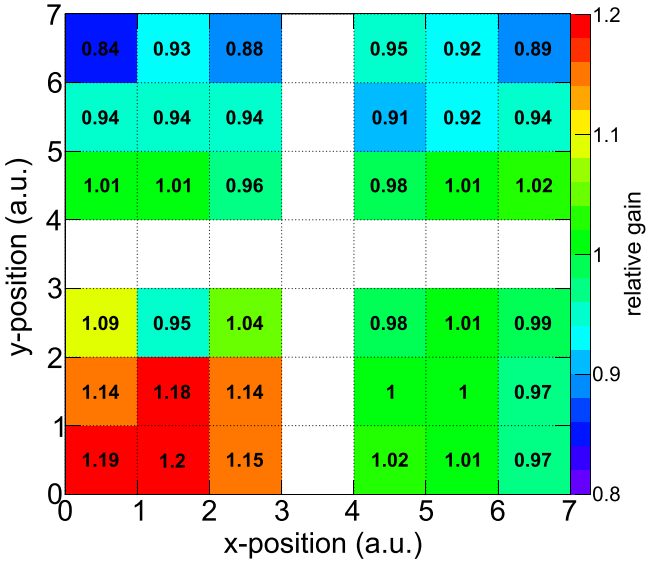

Fig. 11. 2D mapping of relative gain distribution in 36 zones of the GEM detector at an applied voltage of 4400 V.

detector at an applied voltage of 4400 V. The gain has a mean value of 10030 at this voltage with a RMS of 8.8%. As a graphical representation, the relative gain of the detector measured on each zone, has been plotted in Fig. 11 after normalising to the mean value. The gain uniformity result is in good agreement with literature [21]. The energy resolutions obtained for each of the 36 zones at 4400 V is shown in Fig. 12. The mean value of the energy resolution (FWHM) is 21% with a RMS of 6.7%.

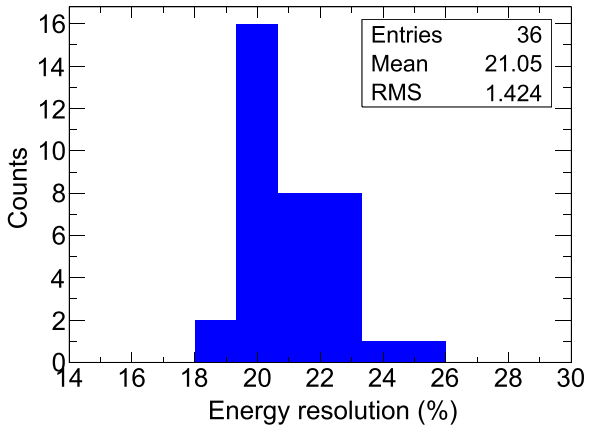

Fig. 12. Distribution of energy resolution values for the 36 zones of the GEM detector at an applied voltage of 4400 V.

6. Summary and outlook

A detailed study of a $10 \times 10\,\mathrm{cm}^2$ triple GEM detector filled with a gas mixture of $Ar+CO_2$ of 70:30 and 90:10 proportions has been performed. Tests were conducted using cosmic rays trigger, a ^{106}Ru-Rh β-source and a ^{55}Fe X-rays source. A plateau in the efficiency around ~95% has been obtained at different operating voltages for the two $Ar+CO_2$ gas mixtures. The energy resolution of the detector was measured to be around 20% for FWHM around the plateau region. A time resolution of ~10 ns has been achieved with the Ar/CO_2 70:30 gas mixture.

Uniformity in gain and energy resolution of the detector have been studied by dividing the detector in 7×7 zones and observing the response to a ^{55}Fe source for each zone separately. The RMS variations of gain and energy resolution are 8.8% and 6.7%, respectively over the entire area. This gain fluctuations can be used in simulations in order to quantify the overall detector response in experiments. The method described in this paper of measuring uniformity in detector gain gives a quantitative account of these parameters, and will prove to be very useful for quality assurance checks for large area GEM detectors.

Acknowledgment

RNP acknowledges the receipt of UGC-NET Fellowship and SB acknowledges the support of DST-SERB Ramanujan Fellowship. YPV thanks Indian National Science Academy, New Delhi for the Senior Scientist position. RNP acknowledges valuable discussions with Rob Veenhof and Dariusz Miskowiec.

References

[1] F. Sauli, Nucl. Instrum. Methods A 386 (1997) 531.
[2] F. Sauli, Nucl. Instrum. Methods A 805 (2016) 2.
[3] G. Bencivenni, et al., Nucl. Instrum. Methods A 488 (2002) 493.
[4] M. Alfonsi, et al., Nucl. Instrum. Methods A 525 (2004) 17.
[5] M. Ball, et al., JINST 9 (2014) C04025.
[6] C. Woody, E. Kistenev, PHENIX Collaboration, J. Phys.: Conf. Ser. (2015), http://dx.doi.org/10.1088/1742-6596/587/1/012054 (012054).

[7] Huan Zhong Huang, STAR Collaboration, Nucl. Phys. A (2013) 921c (904–905).
[8] ALICE Collaboration, Technical Design Report for the Upgrade of the ALICE Time Projection Chamber, ALICE-TDR-016, CERN-LHCC-2013-020, March 3 2014.
[9] Piotr Gasik, ALICE Collaboration, Nucl. Instrum. Methods A 845 (2017) 222.
[10] CMS Collaboration, CMS Technical Design Report for the Muon Endcap GEM Upgrade, CMS-TDR-013, CERN-LHCC-2015-012.
[11] D. Abbaneo, CMS Collaboration, JINST 10 (2015) C03039.
[12] A.K. Dubey, et al., Nucl. Instrum. Methods A 718 (2013) 418.
[13] S. Biswas, et al., Nucl. Instrum. Meth. A 718 (2013) 403.
[14] R.P. Adak, et al., Nucl. Instrum. Methods A 846 (2017) 29.
[15] T. Behnke, et al., arXiv:1306.6329v1.
[16] G. Croci, et al., Nucl. Instrum. Methods A 712 (2013) 108.
[17] R.N. Patra, et al., Nucl. Instrum. Methods A. 824 (2016) 501.
[18] A. Bressan, et al., Nucl. Instrum. Methods A 845 (1999) 262.
[19] M. Abi Akl, et al., Nucl. Instrum. Methods A 832 (2016) 1.
[20] Y. Maghrbi, O. Bouhali, Seventh International Conference on Sensing Technology (ICST), http://dx.doi.org/10.1109/ICSensT.2013.6727768, page(s): 833.
[21] F. Simon, et al., IEEE Trans. Nucl. Sci. 54 (2007) 2646.